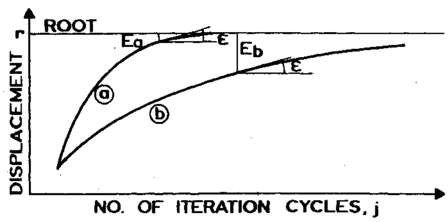

Fig. 2 Examples of slow and fast convergence.

slightly preferable since the other norms yield more of an average bound instead of an absolute bound for all displacement components.

Integrated Norm Criterion

The ε-vector as defined in Eq. (1) does in fact represent the change in displacements during one iteration cycle and it is not an expression of the distance between the present iterate and the true root. As shown in Fig. 2, two cases with the same $\|\varepsilon\|$ (represented by the slope of the curves) may have different total error E_a and E_b. However, an expression for the total error may be obtained taking the integral

$$E_{(j)} \leqq \int_{n=j}^{\infty} \|\varepsilon\| \, dn \tag{6}$$

where n is the iteration cycle.

Since it was demonstrated that the convergence is linear in a semilogarithmic plot, $\|\varepsilon\|$ can be approximated by

$$\|\varepsilon\| \simeq e^{\alpha-\beta n} \quad \text{or} \quad \log\|\varepsilon\| \simeq \alpha - \beta n \tag{7}$$

The coefficients α and β can be obtained by using two of the known values of the curve or by determining a "best fit" through previous values. Substituting Eq. (7) into Eq. (6) and carrying out this extrapolated integration yields

$$E_{(j)} \leqq \frac{1}{\beta} e^{\alpha-\beta j} \tag{8}$$

The use of such an integrated maximum norm for one case of fast convergence and one case of slow convergence is demonstrated in Fig. 3. Thus, at cycle j, $E_{(j)}$ represents the sum of $\|\varepsilon\|_\infty$ at all subsequent cycles. Note that in case of slow convergence $E_{(j)}$ is larger than $\|\varepsilon\|_\infty$ whereas the opposite is true for fast convergence. The integrated norm therefore gives a more true picture of the total error. It may result in a overestimation of the true error when the convergence is oscillatory. However, the convergence stabilizes to a monotonic scheme in almost all cases.

In problems of structural stability, the load-deflection curve rapidly changes character at various levels of loading. As a rule, the convergence is slow in regions of low tangential stiffness. In such regions it usually is not necessary to carry out the iteration to a complete convergence, the difference between the true and the computed load-deflection curve will be small anyway. Unless an absolute error bound is required, the convergence criteria based

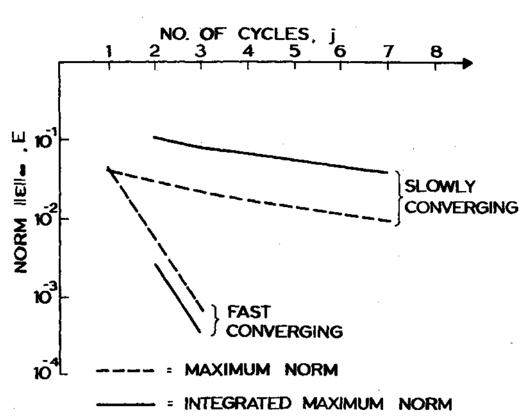

Fig. 3 Integrated error norm.

on Eqs. (2, 3 or 4) and Eq. (5) will in such cases work very well for practical purposes.

Conclusion

A discussion of several convergence criteria for the iterative solution of nonlinear structural problems has been given. In many cases, it is most efficient and accurate to base the convergence criterion merely on displacement quantities. Three alternative norms to be used in such a criterion have been suggested; all of them turn out to be highly useful for practical applications. A convergence criterion based on an extrapolated integration of these norms has also been proposed. This criterion should be used when an absolute bound on the error is desired.

References

[1] Bergan, P. G., "Nonlinear Analysis of Plates Considering Geometric and Material Effects," Ph.D. dissertation, March 1971, University of California, Berkeley, Calif.

[2] Isaacson, E. and Keller, H. B., *Analysis of Numerical Methods*, Wiley, New York, 1966.

Heat Transfer at Reattachment of a Compressible Flow over a Backward Facing Step with a Suction Slot

Demetri P. Telionis*
Virgina Polytechnic Institute and State University, Blacksburg, Va.

Base-flow problems have been extensively studied in the last two decades by both analytical and experimental techniques. Yet the difficulty of such problems has forced the investigators to treat separately the regions of separation, reattachment, recirculating flow, free shear layer and outer flow, and match the individual solutions along the relevant interfaces. The analysis becomes even more complex if $\delta/h \sim 1$ because then the whole recirculating flow is well within the region of influence of viscosity and hence the inviscid core is eliminated. In this case the regions of separation and reattachment overlap and the expansion of the compressible flow is immediately followed by recompression. This is based on experimental evidence[1] that indicate a sudden drop of pressure at the corner followed immediately by an increase without any region of isobaric flow, which is commonly observed for $\delta/h \sim 0.1$ or smaller. The present Note suggests a simplified model for engineering estimates of the heat transfer in the neighborhood of reattachment for the case of supersonic flow over a backward facing step with a suction slot.

It is assumed that the flow properties in the vicinity of reattachment are similar to the properties of stagnation flow. It is also assumed that for $\delta/h \sim 1$ the heat exchanged along the stagnation streamline (SSL) is negligible and therefore the heat transfer at reattachment should be approximately equal to the heat transfer at the point of stagnation of a freestream, with properties those at the stagnation streamline before the expansion (see Fig. 1) which according to Ref. 3 and in the same notation is written as

$$q_R = (T_{os} - T_w)(-S_w'/S_w)(k/x)(Re_x)^{1/2} \{[(m+1)/2] \, d \ln X / d \ln x\}^{1/2} \tag{1}$$

Received Febraury 7, 1972. This work was partially supported by NASA Grant NGR-47-004-070. The contribution of J. A. Schetz is acknowledged for some initial basic ideas.

Index categories: Boundary Layers and Convecture Heat Transfer—Laminar; Sets, Waves, and Vicid-Inviscid Flow Interactions.

* Assistant Professor; Department of Aerospace Engeneering; now with the Department of Engineering Mechanics. Associate Member AIAA.

Notice that an integral of the quantity ρu up to the coordinate y_s defines the amount of mass transferred. Hence the quantity $T_{os} = T_o(y_s)$ appearing in Eq. (1) is an implicit function of the suction rate m defined as

$$\dot{m} = \frac{1}{\rho_1 u_1}\int_o^{y_s} \rho u dy = \frac{T_1}{T_{o1}}\int_o^{\bar{y}_s} \frac{\phi d\bar{y}}{\Lambda - Cr_1{}^2\phi^2} = \left(1 + \frac{\gamma - 1}{2}M_1{}^2\right)\int_o^{\bar{y}_s} \frac{\phi d\bar{y}}{\Lambda - Cr_1{}^2\phi^2} \qquad (2)$$

where $\bar{y} = y/\delta$, $\phi = u/u_1$, $\Lambda = T_o/T_{o1}$ and Cr the Crocco number. Assuming that the appropriate conditions hold, the Crocco integral of the energy equation yields $\Lambda(y) = T_o/T_{o1} = (1 - \Lambda_w)\bar{y} + \Lambda_w$ where $\Lambda_w = T_w/T_{o1}$. With this profile for Λ, a uniform wall temperature and $m = 1$ which corresponds to stagnation by 90°, q_R can be nondimensionalized with the heat transfer at the corner of the step

$$\frac{q_R}{q_s} = \frac{T_{os} - T_w}{T_1 - T_w}\,\frac{\rho_w}{\partial\phi/\partial y|_w}\left(-\frac{S_w'}{S_w}\right)\left(\frac{C}{\mu_s\rho_s}\right)^{1/2} \qquad (3)$$

The crucial point of the present analysis is to define correctly the parameter C which represents the acceleration of the u velocity along the x axis in the absence of the nonslip condition. In the ideal case of freestream stagnation this parameter is estimated as the inner limit of the outer inviscid solution. Yet in the present case the whole region is influenced by viscosity and there is no outer inviscid flow in the aforementioned sense. The proper outer flow should therefore be the viscous flow with the same configuration of streamlines and a symmetry condition imposed on the x axis instead of the nonslip condition. For freestream stagnation, the parameter C can be proved to be proportional to a typical velocity over a typical length, as for example for stagnation on a cylinder, where C is equal to twice the freestream velocity devided by the radius of the cylinder. In the present case we assume that C is proportional to the velocity of the oncoming stream at the SSL divided by the ordinate of the stagnation streamline before the expansion $C = u_D(y_s)/cy_s$. In this way C will depend on the streamline configuration which is a function of the amount of suction. For simplicity a Stokes flow solution was adopted, as suggested by Weiss[4] for the wake-problem of a blunt ended body with base $2h$. This solution does not give a constant velocity gradient at the point of interest but this quantity quickly attains a more or less constant value for practically half the distance to the base wall. For $\delta/h \sim 1$, the recirculating region is fully within the influence of viscosity and hence it seems appropriate to use for the acceleration parameter the preceding constant value of the velocity gradient (for details see Ref. 2)

$$C \equiv \partial u(x_R, 0)/\partial x = u_D(y_s)(az - b)/\Gamma R \qquad (4)$$

where x_R and u_D are defined in Fig. 1 and the quantities $a, b, R, z,$ and Γ are defined in Ref. 4. Therefore $C \equiv \Gamma/4(az - b)\tan\psi$ where ψ the expansion angle and with the assumption of $\mu/\mu_1 = (T/T_1)^\omega$, Eq. (3) becomes

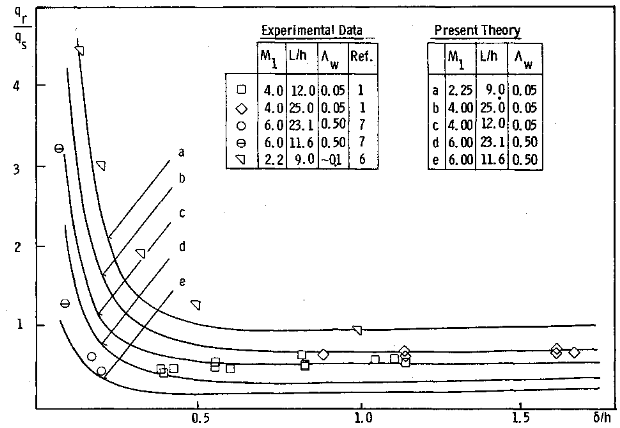

Fig. 2 Heat transfer at reattachment. Comparison of theory with experiment for no mass transfer.

$$\frac{q_R}{q_s} = \frac{T_{os} - T_w}{T_1 - T_w}\,\frac{1}{\partial\phi/\partial\bar{y}|_w}\left(-\frac{S_w'}{S_w}\right)\frac{\rho_w}{\rho_s}\left(\frac{T_1}{T_s}\right)^{(\omega+1)/2}\left[\frac{2\phi Re_{\delta 1}}{c\bar{y}_s}\right]^{1/2} \qquad (5)$$

where $Re_{\delta 1} = u_1\delta/v_1$, $\rho_w/\rho_s = p_w T_s/p_s T_w$ and $T_1/T_s = (\Lambda/\Lambda_w)\cdot(T_w/T_s)$. In these expressions the ratio p_w/p_s was assumed to correspond to 50% recovery of the base pressure at the point of reattachment while the base pressure was estimated according to the correlation of Su and Wu.[5] The ratio T_s/T_w was calculated through the energy equation

$$\frac{T_s}{T_w} = (1/\Lambda_w + 1)y_s/\delta + 1 - \frac{\gamma - 1}{2}\,\frac{M_1{}^2\phi^2}{2\Lambda_w\{1 - [(\gamma - 1)/2]M_1{}^2} \qquad (6)$$

For the flow expansions encountered in practice and along streamlines close to the edge of the boundary layer, the velocity experiences very small changes. As a result it appears that for high-mass transfer rates, $T_{os} - T_w$ is a reasonable choice for the numerator of Eq. (1). It is known that viscous entrainment though accelerates the flow along streamlines close to the wall. In fact for $y_s = h$ the flow is accelerated along the DSL from zero to $\phi_D(h)$† which for the conditions assumed in Ref. 4 and with a constant A included to allow for adjustments by comparison to experiments, reads $\phi_D(h) = [1 + AK\delta/h]^{-1}$. It was then assumed that the above correction to the velocity profile is linear with y and vanishes at $y_s = h + \delta$ and the corresponding increments of the kinetic energy were superimposed on the values of T_{os}. In this way it was possible to estimate q_R/q_s for no mass transfer, using the values of $-S_w'/S_w$ suggested in Ref. 3 and a Blasius velocity profile. Comparison of the present results with available experimental data for no mass transfer is depicted in Fig. 2. The present method correctly predicts a sharp decrease of the heat-transfer ratio with increasing δ/h for $\delta/h < 0.5$ and a mild increase for $\delta/h > 1$, as reported in Ref. 1. In Fig. 3‡ the heat transfer in the neighborhood of stagnation is plotted against the mass transfer rate $\dot{m}$ and parametrized with the wall temperature

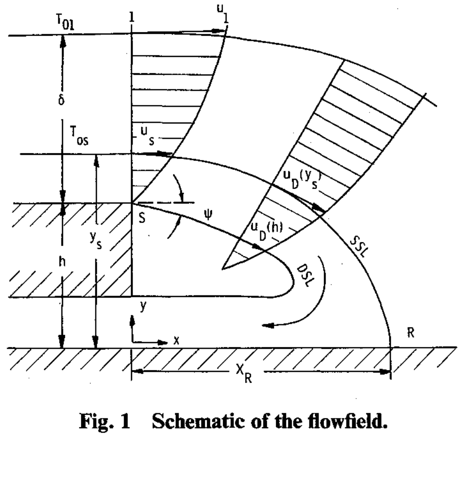

Fig. 1 Schematic of the flowfield.

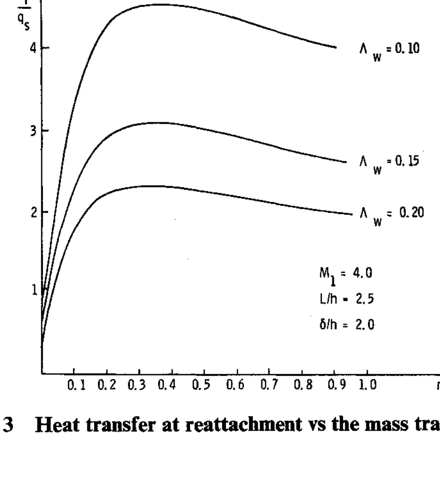

Fig. 3 Heat transfer at reattachment vs the mass transfer rate.

parameter Λ_w. It is noted here that for the time being there are no available experimental data with which to compare for the case of suction and δ/h values larger than $\frac{1}{2}$. When such data becomes available it will be possible to adjust some of the characteristic parameters of the problem if needed.

The present method suggests a closed form approximate solution for a rather complex problem, which was demonstrated to give satisfactory agreement with experiments for the case of no mass transfer, and is expected to predict the effect of mass transfer in the case of suction. This method further indicates the parameters that govern the problem namely, the wall temperature ratio Λ_w, the ratio δ/h, the Mach number M_1, the Reynolds number $Re_{\delta 1}$ and the mass transfer rate $\dot{m}$. Note that the parameter $Re_{\delta 1}$ is proportional to $L/h \cdot h/\delta$, where L the distance from the leading edge to separation and therefore L/h could replace $Re_{\delta 1}$. It appears that $Re_{\delta 1}$ should be the appropriate parameter for design purposes where the local conditions and the boundary-layer thickness are known while L/h should be used to compare with experimental data since in the latter case L/h is usually kept constant.

References

[1] Jakubowski, A. K., Kirchner, R. D., Brown, R. D., and Lewis, C. H., "Experimental Investigation of Heat Transfer and Pressure Distribution in Laminar Separated Flows Downstream of a Rearward Facing Step: Part I No Suction," Engineering Report, Virginia Polytechnic Inst., Blacksburg, Va.

[2] Telionis, D. P. and Swean, T. F., "Approximate Methods for the Calculation of the Heat Transfer Behind a Rearward Facing Step with a Suction Slot," Engineering Report, Virginia Polytechnic Inst., Blacksburg, Va.

[3] Cohen, C. B. and Reshotko, E., "Similar Solution for the Compressible Laminar Boundary Layer with Heat Transfer and Pressure Gradient," Rept. 1293, 1950, NACA.

[4] Weiss, R., "The Near Wake of a Wedge," Research Rept. 197, 1964, Avco Everett Research Lab., Everett, Mass.

[5] Su, W. M. and Wu, J. M., "Base Pressure Correlation in Supersonic Flow," *AIAA Journal*, Vol. 9, No. 7, July 1970, pp. 251–255.

[6] Rom, J. and Seiginer, A., "Laminar Heat Transfer to a Two-Dimensional Backward Facing Step from the High Enthalpy Flow in the Shock Tube," *AIAA Journal*, Vol. 2, No. 2, Feb. 1964, pp. 251–255.

[7] Holloway, P. F., Sterett, J. R., and Creekmore, H. S., "An Investigation of Heat Transfer within Regions of Separated Flow at a Mach Number of 6.0," TN D-3074, 1965, NASA.

† Note that in the present notation y is defined as the ordinate of a streamline before expansion, it is therefore introduced here a modified stream function.

‡ Note added in proof: Dr. Jakubowski has recently informed the author that some initial experimental result indicate that q_r/q_s might be a little overestimated in Fig. 3. Yet the inability to measure accurately the mass transfer rate and the small number of experimental points would not permit a comparison.

Particle Charging behind Shock Waves in Suspensions

B. M. Shirley* and J. W. Sheldon†
Florida State University, Tallahassee, Fla.
and
S. C. Kranc
University of South Florida, Tampa, Fla.

Received February 8, 1972; revision received March 20, 1972. Research supported in part by NSF Grant GK 5343.

Index category: Multiphase Flows.

* Research Assistant.

† Associate Professor, School of Engineering Science.

Assistant Professor, Department of Structures, Materials, and Fluids. Associate Member AIAA.

Nomenclature

J = particle flux
L = velocity equilibration length
r = radius
R = rate of collision
U = particle velocity
v = gas velocity
X = distance behind shock

Subscripts
d = downstream
i = particle class index
m = maximum
u = upstream
μ = viscosity
ρ = density

DURING an experimental investigation of shock structure in gases containing dust suspensions, substantial electrical signals associated with the shock wave were observed. A series of qualitative experiments was conducted to determine the mechanism producing these signals.

These experiments were conducted in an ordinary pressure driven shock tube made of aluminum tubing 5.7 cm in diameter and operated in a vertical position. A measured mass of glass particles supplied by Heat Systems-Ultrasonics and having a nominal size distribution of 5μ diameter was introduced into the test section while a gentle gas flow from below was maintained to keep the suspension uniform. Maximum densities obtained in this manner were approximately 10^7 particles/cm^3, calculated by assuming an even distribution of particles in the test section. The tube was instrumented with a piezoelectric pressure transducer and an electrical probe at an observation station located 71 cm from the diaphragm. The probe consisted of a short length of bare wire aligned in the flow by a grounded shield. The voltage from probe to ground and the pressure trace were recorded simultaneously on a dual channel oscilliscope.

In the first experiment, a relatively weak shock ($M = 1.15$) was propagated in the test section. The oscilliscope traces presented in Fig. 1a demonstrate the development of a voltage signal behind the shock wave as it passes through the suspension. Two different loadings are shown. Similar signals were observed for other particulate matter such as ammonium chloride and tin oxide. In a second experiment, a rarefaction wave was propagated in the test section through the suspension by evacuating the chamber on the other side of the diaphragm until rupture occurred. Figure 1b shows the pressure and voltage traces during the passage of a rarefaction wave. No signals were observed when particles were not present in the test section during the passage of a wave.

We considered several possible causes for these signals. While the particles were not intentionally given an initial charge, all dusts do have some residual charge but this is generally quite small. Particle collisions with the probe are ruled out since

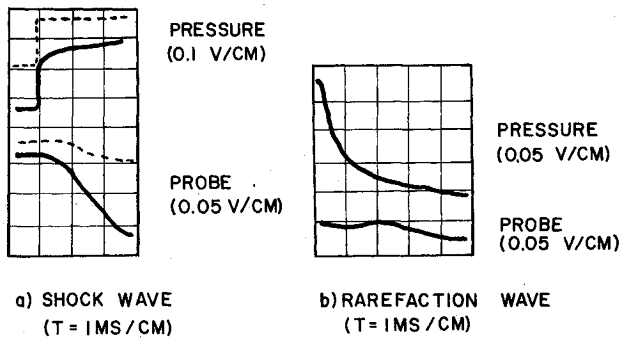

Fig. 1 Comparison of electrical signals for a) shock wave and b) rarefaction wave. Velocities behind waves are approximately 80 m/sec and 276 m/sec, respectively. Particle loading effects decrease actual velocities and degrade pressure traces as shown. (Solid lines indicate particle loading 10^7/cm^3, dotted line indicates 5×10^6/cm^3.)